# Direct product of random unitary matrices: Two-point correlations and fluctuations

Ramgopal Agrawal [*] and Akhilesh Pandey [†]
*School of Physical Sciences, Jawaharlal Nehru University, New Delhi 110067, India*

Ravi Prakash [‡]
*Department of Physics, Motilal Nehru National Institute of Technology Allahabad, Prayagraj 211004, India*

(Received 22 June 2021; accepted 30 August 2021; published 10 September 2021)

We study the ensembles of direct product of $m$ random unitary matrices of size $N$ drawn from a given circular ensemble. We calculate the statistical measures, viz. number variance and spacing distribution to investigate the level correlations and fluctuation properties of the eigenangle spectrum. Similar to the random unitary matrices, the level statistics is stationary for the ensemble constructed by their direct product. We find that the eigenangles are uncorrelated in the small spectral intervals. While, in large spectral intervals, the spectrum is rigid due to strong long-range correlations between the eigenangles. The analytical and numerical results are in good agreement. We also test our findings on the multipartite system of quantum kicked rotors.

DOI: 10.1103/PhysRevE.104.034208

## I. INTRODUCTION

The *circular ensembles* of random unitary matrices were introduced by Dyson [1–3] to study the spectral properties of complex quantum systems. Due to the simplicity, the circular ensembles are advantageous over the *Gaussian ensembles* of Hermitian random matrices. Numerous studies [4–8], including time-periodic quantum chaotic systems, quantum maps, and scattering matrices, have used the random unitary matrices as an appropriate universal model. Depending on the symmetries of the underlying system, the ensembles of random unitary matrices are classified into three universality classes [3,9]. The *circular unitary ensembles* (CUEs) of arbitrary unitary matrices are appropriate to model a system without the time-reversal symmetry. When the system with integer spin preserves the time-reversal and rotational symmetries, *circular orthogonal ensembles* (COEs) of symmetric unitary matrices are appropriate. For systems with half-integer spin, which preserves the time-reversal but the rotational symmetry no longer holds, one should use *circular symplectic ensembles* (CSEs) of self-dual unitary quaternion matrices. The eigenangle spectrum of each universality class possesses nonzero level repulsion unique in itself.

In the field of random matrix theory (RMT), the main interest lies in the local fluctuation properties of the spectrum. Such properties are independent of the global constraints imposed by the average level density and exhibit universal features. Before investigating the local properties, one first unfolds the spectrum by transforming the average level density to unity. The local properties of the unfolded spectrum are then analyzed by the two-point statistical measures, e.g., *number variance statistics* $\Sigma^2(r)$; here $\Sigma^2(r)$ is the variance of the number of levels in an interval of size $rD$ and $D$ is the average level spacing. It is a direct measure of the rigidity of the spectrum. For uncorrelated spectrum, $\Sigma^2(r)$ grows linear with interval size $r$ while, for the spectrum from RMT-ensemble, it has logarithmic increment with $r$. This slow growth (logarithmic) indicates the presence of level correlations. The level-spacing distribution $P(s)$ is another useful measure. It has *Poissonian* behavior for uncorrelated spectrum and *Wigner-Dyson* for RMT-spectrum.

Today, random matrices are widely used in diverse areas of physics and sciences. While the classical RMT-ensembles (Gaussian or circular) have been a stepping stone for the development of RMT, they only serve as pure phenomenological models. We often require the generalized ensembles of random matrices to model a complicated system. This paper will discuss such an ensemble composed by the direct product of random unitary matrices. The ensembles of the direct product of random matrices are useful to model the spatially extended systems in the fields of quantum information and graph networks [10,11]. Their extension in terms of transition ensembles have recently found applications in quantum entanglement [12–14]. Despite the good physical relevance, there are only a few preliminary works [15,16] available in this direction. Moreover, these works focus on the short-range spectral fluctuations only. Our aim in the present paper is to provide a detailed account of the two-point spectral correlations in the ensembles of direct product of $m$ independent random unitary matrices of size $N$ drawn from a given circular ensemble. We present the analytical results for the direct product of $m$ independent random unitary matrices in general and support them numerically for $m = 2$. We also formulate a multipartite system of *quantum kicked rotors* (QKRs) to verify our results. The spectral statistics of QKRs is consistent with those of COEs/CUEs [17,18]. Therefore, we expect that their multipartite version should serve as a test bed for direct product ensembles. The interesting observations of our paper are as follows:

[*]ramgopal.sps@gmail.com
[†]apandey2006@gmail.com; ap0700@mail.jnu.ac.in
[‡]raviprakash.sps@gmail.com; ravi.prakash@mnnit.ac.in

 

(1) The eigenangles of the spectrum obtained from direct product of $m$ independent random unitary matrices are uncorrelated in the small spectral intervals, as characterized by the linear growth of number variance and Poissonian behavior of spacing distribution.

(2) The number variance for large spectral intervals shows saturation behavior, which implies that the spectrum is rigid, i.e., there are strong correlations between the distant eigenangles. The level-spacing distribution is non-Poissonian for large spacings.

(3) The spectral statistics of the multipartite system of QKRs is in good agreement with our findings for direct product ensembles.

This paper is organized as follows. First, in Sec. II, we briefly discuss the random unitary matrices. In Sec. III, the ensembles of direct product of random unitary matrices are described. We discuss the spectral properties of the direct product matrices in Sec. IV. In Sec. V, we provide our numerical results. Further, in Sec. VI, we explore the multipartite system of QKRs. Finally, in Sec. VII, we give a summary and discuss our results obtained so far in the paper.

## II. RANDOM UNITARY MATRICES

For the circular ensembles of random unitary matrices, the joint probability distribution (JPD) of eigenangles $\{\theta_i\}_{i=1,2,..,N}$ is given by [2,3]

$$\mathcal{P}_{N,\beta}(\theta_1, ..., \theta_N) = C_{N,\beta} \prod_{j>k} \left|e^{i\theta_j} - e^{i\theta_k}\right|^\beta, \tag{1}$$

where $C_{N\beta}$ is the normalization constant, $N$ is the dimensionality of the matrices, and $\beta$ is the degree of level repulsion with $\beta = 1$ for orthogonal, 2 for unitary, and 4 for symplectic class. Since JPD $\mathcal{P}_{N,\beta}$ depends only on the differences between the eigenangles, circular ensembles are homogeneous. In particular, the ensemble-averaged level-density

$$\begin{aligned} R_1(\theta) &= \overline{\rho(\theta)} \\ &= \int_0^{2\pi}\int_0^{2\pi} .... \int_0^{2\pi} \left\{\sum_i \delta[\theta - \theta_i]\right\} \\ &\quad \times \mathcal{P}_{N,\beta}(\theta_1, ..., \theta_N)\, d\theta_1 d\theta_2 .... d\theta_N \end{aligned} \tag{2}$$

is constant ($= N/2\pi$); here the bar denotes the ensemble average. The eigenangle spectrum is then unfolded simply by multiplying the constant $N/2\pi$.

The two-point correlations in the eigenangle spectrum are characterized by the two-point correlation function of level density [2],

$$K(\theta, \theta') = \overline{\rho(\theta)\rho(\theta')}, \tag{3}$$

with the normalization condition

$$\int_0^{2\pi}\int_0^{2\pi} K(\theta, \theta')\, d\theta d\theta' = N^2. \tag{4}$$

The connected version of the two-point function is sometimes more useful and is calculated from the disconnected one by subtracting the product of two average level densities:

$$K_c(\theta, \theta') = K(\theta, \theta') - R_1(\theta)R_1(\theta'). \tag{5}$$

Since the eigenangles of a unitary matrix lie on the unit circle ($0 < \theta_i < 2\pi$), the level density of the spectrum can be expressed in terms of Fourier expansion,

$$\rho(\theta) = \frac{1}{2\pi} \sum_{p=-\infty}^{\infty} M_p\, e^{ip\theta}, \tag{6}$$

where $M_p = \mathrm{Tr}\, U^p$ are the traces of $p$th power of the random unitary matrix $U$ drawn from a circular ensemble and the index $p$ is an integer ($p = 0, \pm1, \pm2, ....$).

By use of Eq. (6), $K_c$ can be written in terms of $M_p$ as

$$K_c(\theta, \theta') = \frac{1}{(2\pi)^2} \sum_{p\neq 0} \overline{|M_p|^2}\, e^{ip(\theta-\theta')}, \tag{7}$$

with the identity $\overline{M_p M_q} = \delta_{p,-q}\overline{|M_p|^2}$ due to homogeneity of the spectra. The Fourier coefficient of $K_c(\theta, \theta')$, also known as the *spectral form factor*, is given as [2]

$$\begin{aligned} C(p, q) &= \int_0^{2\pi}\int_0^{2\pi} e^{ip\theta} e^{iq\theta'} K_c(\theta, \theta')\, d\theta d\theta' \\ &= \overline{M_p M_q} - \overline{M_p}\,\overline{M_q};\ \ p, q = 0, \pm1, \pm2, .... \end{aligned} \tag{8}$$

which is nonzero for $p + q = 0$. We will denote it as $C(p)$ in the paper.

$C(p)$ is useful to calculate two-point fluctuation measures. The exact results of $C(p)$ for finite $N$ are derived in Ref. [19]. For $\beta = 1$, it is given as

$$\begin{aligned} C(p) &= 2|p| - |p| \sum_{\mu=(N-1)/2-|p|+1}^{(N-1)/2} \frac{1}{\mu + |p|}, \quad |p| \leqslant N, \\ &= 2N - |p| \sum_{\mu=-(N-1)/2}^{(N-1)/2} \frac{1}{\mu + |p|}, \quad |p| \geqslant N. \end{aligned} \tag{9}$$

For $\beta = 2$, $C(p)$ is

$$\begin{aligned} C(p) &= |p|, \quad |p| \leqslant N, \\ &= N, \quad |p| \geqslant N. \end{aligned} \tag{10}$$

And, for $\beta = 4$, it is

$$\begin{aligned} C(p) &= \frac{|p|}{2} + \frac{|p|}{4} \sum_{\mu=N-|p|+\frac{1}{2}}^{N-\frac{1}{2}} \frac{1}{\mu}, \quad |p| \leqslant 2N, \\ &= N, \quad |p| \geqslant 2N. \end{aligned} \tag{11}$$

In the next section, we describe the direct product of random unitary matrices and detail the two-point function results.

## III. DIRECT PRODUCT OF RANDOM UNITARY MATRICES

For the composed ensembles defined by the direct product of random unitary matrices, we consider $m$ random unitary matrices $U_1, U_2, ...., U_m$ each of size $N$, with eigenangles $\{\theta_{i_1}^{(1)}\}_{i_1=1,2,..,N}$, $\{\theta_{i_2}^{(2)}\}_{i_2=1,2,..,N}$,...., $\{\theta_{i_m}^{(m)}\}_{i_m=1,2,..,N}$, respectively. The direct product of these $m$ matrices is defined as

$$\widetilde{U} = U_1 \otimes U_2 \otimes .... \otimes U_m, \tag{12}$$

where the size of the matrix $\widetilde{U}$ is $N^m$. The eigenvalues of $\widetilde{U}$ are obtained from the product of the eigenvalues of component matrices $U_1, U_2, ....$ Therefore, the eigenangles of the matrix $\widetilde{U}$ are

$$\Theta_{i_1 i_2 .. i_m} = \theta^{(1)}_{i_1} + \theta^{(2)}_{i_2} + .... + \theta^{(m)}_{i_m} \bmod 2\pi, \tag{13}$$

where indices $i_1, i_2, .., i_m = 1, 2, ...., N$. The ensembles of the direct product of random unitary matrices each pertaining to a given circular ensemble can be classified analogous to circular ones, i.e., ensemble of direct product of COE matrices, ensemble of direct product of CUE matrices, and ensemble of direct product of CSE matrices.

In this paper, we are considering a special case where the component matrices $\{U_i\}$ are independent of each other. The direct product of identical matrices can also be explored on the same ground, but we do not find any interesting feature to discuss them here.

The advantage of the direct product of independent matrices is that the eigenangles from independent matrices are uncorrelated to each other and, therefore, the calculation of the two-point function results becomes easier. First, the average level density for the direct product of $m$ independent random unitary matrices is obtained from the following convolution relation:

$$R_1^{m\otimes}(\Theta) = \int_0^{2\pi}\int_0^{2\pi} .... \int_0^{2\pi} \{R_1(\theta^{(1)}) R_1(\theta^{(2)}) .... R_1(\theta^{(m)}) \times \delta[\Theta - (\theta^{(1)} + \theta^{(2)} + .... + \theta^{(m)})]\} \times d\theta^{(1)} d\theta^{(2)} .... d\theta^{(m)}, \tag{14}$$

where $R_1(\theta^{(1)}), R_1(\theta^{(2)}), ...$ are the average level-densities for different random unitary matrices. Since $\Theta$ is periodic with period $2\pi$, we have $\delta(\Theta) = \delta(\Theta + 2\pi)$. We replace $\delta$-term by its Fourier series expansion,

$$\delta\left(\Theta - \sum_i \theta^{(i)}\right) = \frac{1}{2\pi}\sum_{p=-\infty}^{\infty} \exp\left(ip\left(\Theta - \sum_i \theta^{(i)}\right)\right), \tag{15}$$

and substitute $R_1(\theta^{(i)}) = N/(2\pi)$ in Eq. (14). After evaluating integrals over the $\theta^{(i)}$ followed by the summation over integer $p$, we get

$$R_1^{m\otimes}(\Theta) = \frac{N^m}{2\pi}. \tag{16}$$

We further write the disconnected two-point function of level density for the direct product of $m$ independent random unitary matrices, $K^{m\otimes}(\Theta, \Theta')$ as

$$K^{m\otimes}(\Theta, \Theta') = \int_0^{2\pi}\int_0^{2\pi} .... \int_0^{2\pi} \{K(\theta^{(1)}, \theta'^{(1)}) K(\theta^{(2)}, \theta'^{(2)}) .... K(\theta^{(m)}, \theta'^{(m)}) \times \delta[\Theta - (\theta^{(1)} + \theta^{(2)} + .... + \theta^{(m)})]\, \delta[\Theta' - (\theta'^{(1)} + \theta'^{(2)} + .... + \theta'^{(m)})]\} d\theta^{(1)} d\theta'^{(1)} d\theta^{(2)} d\theta'^{(2)} .... d\theta^{(m)} d\theta'^{(m)}, \tag{17}$$

where $K(\theta^{(1)}, \theta'^{(1)}), K(\theta^{(2)}, \theta'^{(2)}), ...$ are the (disconnected) two-point functions for the component matrices.

By using Eqs. (3) and (6) for the $K(\theta^{(i)}, \theta'^{(i)})$, and Eq. (15) for $\delta$ terms, we get

$$K^{m\otimes}(\Theta, \Theta') = \frac{1}{(2\pi)^2}\sum_{p=-\infty}^{\infty}\left[\overline{|M_p|^2}\right]^m e^{ip(\Theta-\Theta')}, \tag{18}$$

where $\overline{|M_p|^2}$ are the ensemble-averaged squared-in-modulus traces for the circular ensemble. The connected two-point function is given by

$$K_c^{m\otimes}(\Theta, \Theta') = \frac{1}{(2\pi)^2}\sum_{p\neq 0}\left[\overline{|M_p|^2}\right]^m e^{ip(\Theta-\Theta')}. \tag{19}$$

It is straightforward to see from Eq. (19) that the Fourier coefficient of $K_c^{m\otimes}$ (spectral form factor) is

$$C^{m\otimes}(p) = [C(p)]^m, \tag{20}$$

where $C(p)$ is the spectral form factor of random unitary matrices [Eqs. (9)–(11)]. In the next section, we will exploit the above relation to analyze the spectral properties of the direct product of $m$ independent random unitary matrices.

## IV. LEVEL CORRELATIONS AND FLUCTUATIONS

To investigate the local spectral properties, one often uses the rigidity measure, namely, the number variance. For the eigenangle spectrum of the direct product of $m$ independent random unitary matrices, it can be found from the two-point function of level density as [2]

$$\Sigma^2(\Delta, \epsilon) = \int_{\epsilon-\Delta/2}^{\epsilon+\Delta/2}\int_{\epsilon-\Delta/2}^{\epsilon+\Delta/2} K_c^{m\otimes}(\Theta, \Theta')\, d\Theta d\Theta', \tag{21}$$

where $\Delta$ is the width and $\epsilon$ is the location of the spectral interval. Denoting $z = \Theta - \Theta'$ and $s = (\Theta + \Theta')/2$, we see from Eq. (19) that $K_c^{m\otimes}(\Theta, \Theta') = K_c^{m\otimes}(z)$, i.e., $K_c^{m\otimes}$ depends only on the difference $z$. It gives

$$\Sigma^2(\Delta, \epsilon) = \Sigma^2(\Delta) = 2\int_0^{\Delta}(\Delta - |z|)\, K_c^{m\otimes}(z)\, dz. \tag{22}$$

This property reflects the stationarity of the level statistics in the direct product ensembles.

By using the Fourier expansion of $K_c^{m\otimes}$ [Eq. (19)], we have for the unfolded spectrum

$$\Sigma^2(r) = \sum_{p=-\infty}^{\infty} C^{m\otimes}(p)\frac{\sin^2(\pi pr/N^m)}{(\pi p)^2}, \tag{23}$$

where $r = R_1^{m\otimes}\Delta$ is the unfolded width of the spectral interval. Note that $\Sigma^2(r) = \Sigma^2(N^m - r)$ due to the periodicity of the spectrum. We further discuss the fluctuation properties for the small and large spectral intervals.

### A. Small spectral intervals

The eigenangles of the direct product spectrum observe the sum of eigenangles from different random unitary matrices with modulo-$2\pi$ [Eq. (13)]. Because of that, a degree of randomness arises in the small spectral intervals. Similar behavior is also recovered when one superposes many independent spectra [20]. This fact can be understood from the behavior of form factor $C^{m\otimes}(p)$ at large $p$. The form factor of circular ensembles $C(p)$ goes to $N$ for $|p| \gtrsim N$, where $|p| = N$ is the timescale conjugate to the average level spacing $D$ of the spectrum [21]. It gives $C^{m\otimes}(p) \simeq N^m$ for $|p| \gtrsim N$ [see Eq. (20)]. Then, from the expression in Eq. (23), the number variance

$$\Sigma^2(r) \sim N^m \sum_{p=-\infty}^{\infty} \frac{\sin^2(\pi pr/N^m)}{(\pi p)^2} = r \tag{24}$$

for intervals of size $r \ll N^{m-1}$. It implies that the eigenangles are uncorrelated in the small spectral intervals. Obviously, the width of the interval is extended for large $N$ or $m$. In Sec. V, we will numerically verify the above linear growth of $\Sigma^2(r)$.

### B. Large spectral intervals

Contrary to the uncorrelated eigenangles in the small intervals, we expect the development of the strong level repulsion in the large intervals. The reason is the global rigidity of the spectrum. In circular ensembles, level repulsion arises for $r \gtrsim 1$ wherein $\Sigma^2(r)$ grows logarithmic (slowly) with $r$. The integrable systems, which are generic to Poisson statistics, also exhibit strong rigidity at large energy scales [22,23].

The behavior of form factor $C^{m\otimes}(p)$ at small $p$ is crucial for the local fluctuations in the large spectral intervals. With the increase in $p$ from zero, $C^{m\otimes}(p)$ increases from zero with the $m$th power of $C(p)$, where $C(p)$ is the form factor of random unitary matrices. Therefore, when $m > 1$, $C^{m\otimes}(p)$ has suppressed increase at small $p$ and steeper increase around $|p| \simeq N$. This regime of small $p$, where the form factor has suppressed increase, indicates the strong two-point correlations between the far-lying eigenangles. We further explain this fact with the help of a model originally proposed for the integrable systems [23,24]. Consider the spectral form factor of the form

$$\mathbb{C}(p) = \begin{cases} 0, & 0 \leqslant |p| \leqslant t \\ L, & t < |p| < \infty. \end{cases} \tag{25}$$

Here, $L$ is the size of the spectrum and $t$ is an integer with $0 \leqslant t < L$. In Fig. 1, we plot $\Sigma^2(r)$ vs $r$ using Eq. (23) for above model. When $t$ is zero, $\Sigma^2(r)$ grows linear at all $r$, yielding the uncorrelated nature of levels in the spectrum. As soon as $t$ becomes nonzero, it grows linear for small intervals but approaches a constant value ($\propto 1/t$) for larger intervals (see inset of the same figure). This saturation of $\Sigma^2(r)$ at large $r$ implies the presence of strong long-range correlations in the spectrum. Since the form factor of the direct product ensembles is suppressed at early times (small $p$), we expect the similar saturation of $\Sigma^2(r)$ to appear therein.

The saturation behavior of number variance has been reported in the studies of several systems [22,25–27]. For the present case, this saturation value can be estimated by averaging out the oscillating part in Eq. (23) over the large spectral intervals. For any saturation behavior in $\Sigma^2(r)$, the resulting series should be convergent. We replace the sine squared term in Eq. (23) by its average over large intervals, 1/2. Thus, we get

$$\Sigma^2_{\rm sat} = \sum_{p=-\infty}^{\infty} C^{m\otimes}(p) \frac{1}{2\pi^2 p^2} \tag{26}$$

for large $r \sim O(N^{m-1})$. The above sum can be calculated with an appropriate cutoff.

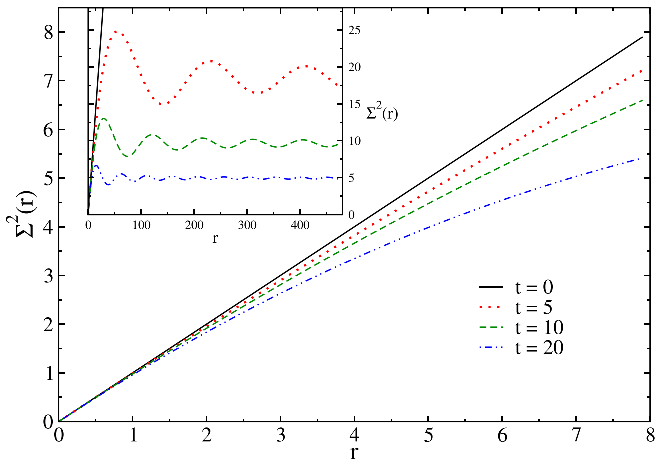


FIG. 1. The plot of number variance $\Sigma^2(r)$ vs interval size $r$ for form factor in Eq. (25) of main text. Inset represents the same data for large $r$.

### V. NUMERICAL STUDY

In the present section, we provide a numerical verification of the results obtained in the previous section. We deal specifically with the ensembles of a direct product of two independent random unitary matrices and investigate the statistical quantities like number variance and spacing distribution.

To obtain the eigenangle spectrum of the direct product, we first generate random unitary matrices from CUEs using QR-decomposition technique [28,29]. The COE and CSE matrices are then obtained using the properties $U' \rightarrow U^T U$ and $U' \rightarrow U^R U$, respectively, with $U$ being the random unitary matrix from CUE, $U^T$ its transpose, and $U^R$ being the dual of matrix $U$ [3,4]. These matrices are diagonalized using standard LAPACK routine [30]. The eigenangles of the direct product of two independent CUE matrices (CUE ⊗ CUE), COE matrices (COE ⊗ COE), or CSE matrices (CSE ⊗ CSE) are obtained by adding the eigenangles of component matrices [see Eq. (13)]. The quantities of interest are then calculated from the obtained eigenangle spectrum.

We calculate the spectral form factor $C^{2\otimes}(p)$ from the relation

$$C^{2\otimes}(p) = \overline{\left|\mathrm{Tr}\,\widetilde{U}^p\right|^2} - \left|\overline{\mathrm{Tr}\,\widetilde{U}^p}\right|^2 = \overline{\left|\sum_j e^{ip\Theta_j}\right|^2} - \left|\overline{\sum_j e^{ip\Theta_j}}\right|^2, \tag{27}$$

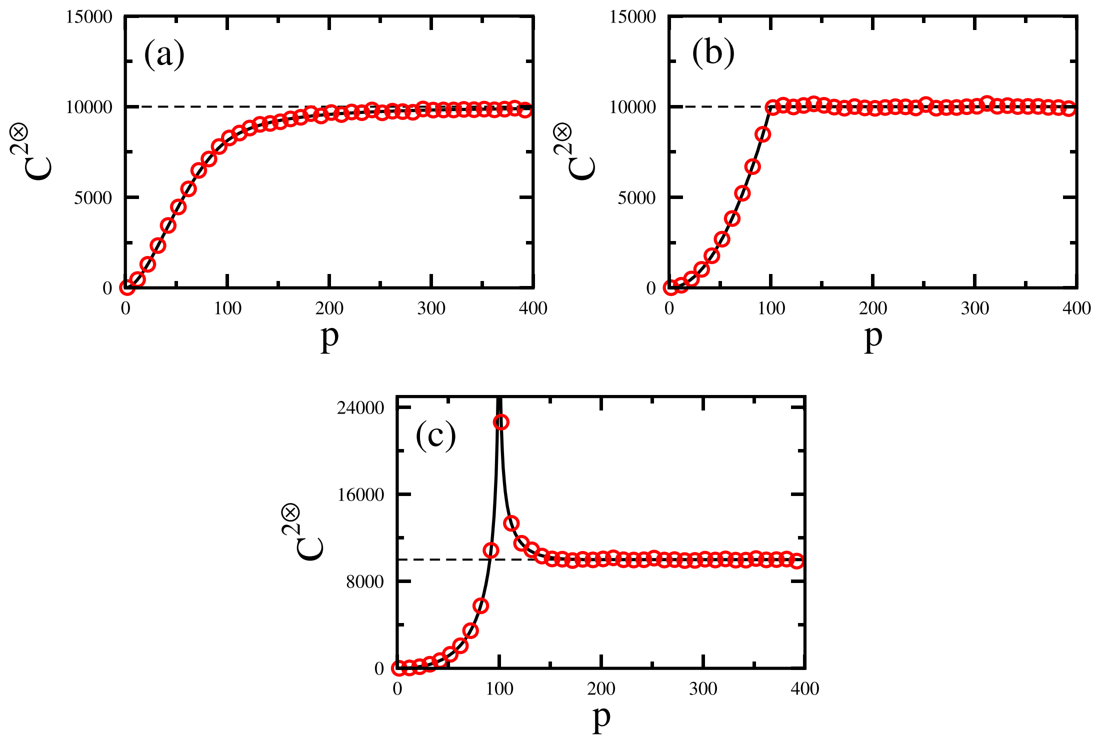


FIG. 2. The plot of form factor $C^{2\otimes}(p)$ vs $p$ for (a) COE $\otimes$ COE, (b) CUE $\otimes$ CUE, and (c) CSE $\otimes$ CSE. The circles denote numerical data. The size of the spectrum is $N^2 = 100^2$. The solid curves in (a)–(c) denote analytical results (see main text). The dashed lines indicate $C^{2\otimes}(p) = N^2$.

where the bar denotes the ensemble average and the matrix $\widetilde{U}$ is the direct product of two random unitary matrices ($\widetilde{U} = U_1 \otimes U_2$).

For number variance, we first unfold the spectrum using unfolding function $(N^2/2\pi)\,\Theta_i$. The number variance is then calculated by taking the variance of the number of eigenangles $n(r)$ in interval size $r$:

$$\Sigma^2(r) = \overline{n^2(r)} - \overline{n(r)}^2. \tag{28}$$

Another important quantity that we calculate is the level-spacing distribution $P_{n-1}(s)$. It is the distribution of spacings between two levels with $n-1$ levels in the middle. This quantity is straightforward to calculate from an increasingly ordered spectrum.

For the numerical results reported in this paper, the size of the single random unitary matrix from COEs and CUEs is taken $N = 100$, while the random unitary matrices of size $2N$ are considered from CSEs. One should note that the eigenangles of matrices from CSE are doubly degenerate. Therefore, we remove the duplicate eigenangles by hand from the spectrum and, in this way, $N$ number of eigenangles are obtained from the diagonalization of the $2N$-sized CSE matrix. The numerical data of the form factor is obtained by averaging over an ensemble of 50 000 spectra. The number variance in an interval of size $r$ is calculated by averaging over 1500 spectra. The level-spacing distribution is calculated from 500 spectra.

### A. Form factor and number variance

The form factor for the direct product of two independent random unitary matrices $C^{2\otimes}(p)$ can be calculated from Eq. (20) as

$$C^{2\otimes}(p) = [C(p)]^2, \tag{29}$$

where the form factor $C(p)$ of circular ensembles (COE, CUE, and CSE) are given by Eqs. (9)–(11). In Figs. 2(a)–2(c), we display the numerical as well as the analytical results of $C^{2\otimes}(p)$ for COE $\otimes$ COE, CUE $\otimes$ CUE, and CSE $\otimes$ CSE. Both have excellent agreement with each other in all three classes. The suppression of $C^{2\otimes}(p)$ at small $p$ is also confirmed.

Further, by substituting $C^{2\otimes}(p)$ in Eq. (23), we calculate the expressions of the number variance for different classes. For COE $\otimes$ COE, it is given as

$$\Sigma^2(r) = 2\sum_{p=1}^{N}\left[2 - \psi\left(\frac{N+1}{2}+p\right) + \psi\left(\frac{N+1}{2}\right)\right]^2 \frac{\sin^2(\pi pr/N^2)}{\pi^2} + 2\sum_{p=N+1}^{\infty}\left[\frac{2N}{p} - \psi\left(\frac{N+1}{2}+p\right) + \psi\left(\frac{1-N}{2}+p\right)\right]^2 \frac{\sin^2(\pi pr/N^2)}{\pi^2}. \tag{30}$$

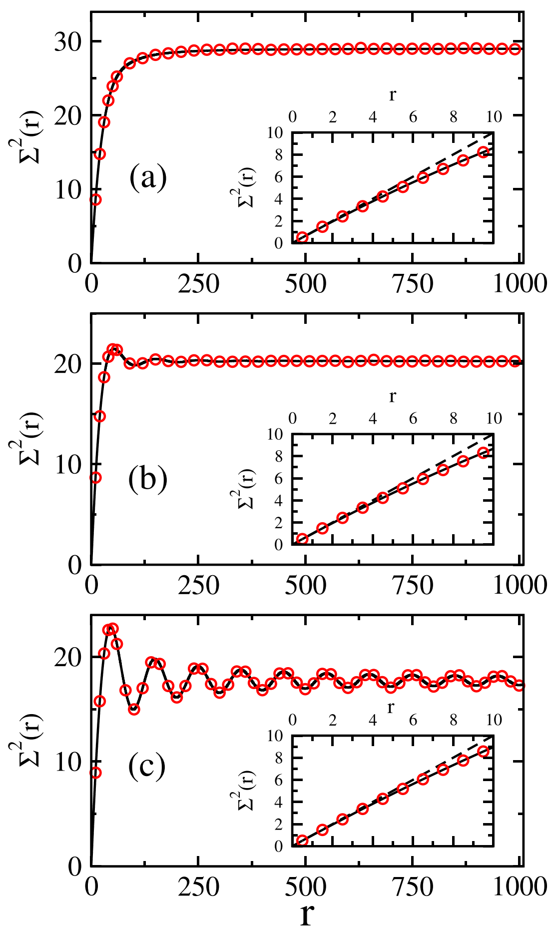


FIG. 3. Number variance $\Sigma^2(r)$ vs interval size $r$ for (a) COE ⊗ COE, (b) CUE ⊗ CUE, and (c) CSE ⊗ CSE. The numerical data is shown by circles. The size of the spectrum is $N^2 = 100^2$. Data for small intervals is shown in insets, where the dashed lines denote $\Sigma^2(r) = r$. The solid curves in both main frame and inset of panels (a)–(c) are plotted using Eqs. (30)–(32), respectively.

The expression for CUE ⊗ CUE is

$$\Sigma^2(r) = 2\sum_{p=1}^{N}\frac{\sin^2(\pi pr/N^2)}{\pi^2} + 2N^2\sum_{p=N+1}^{\infty}\frac{\sin^2(\pi pr/N^2)}{(\pi p)^2}, \tag{31}$$

and for CSE ⊗ CSE, the expression of $\Sigma^2(r)$ is

$$\Sigma^2(r) = \frac{1}{8}\sum_{p=1}^{2N}\left[2+\psi\left(N+\frac{1}{2}\right)-\psi\left(N-p+\frac{1}{2}\right)\right]^2 \times \frac{\sin^2(\pi pr/N^2)}{\pi^2} + 2N^2\sum_{p=2N+1}^{\infty}\frac{\sin^2(\pi pr/N^2)}{(\pi p)^2}. \tag{32}$$

Here $\psi(z)$ is the digamma function $(= -\gamma + \sum_{n=1}^{\infty}[\frac{1}{n} - \frac{1}{n+z-1}])$; $\gamma$ is Euler's gamma. For $N \to \infty$, the summations in the above expressions can be replaced by the integrals over a variable $k$ such that $p/N^2 \to k$. However, for finite $N$, one has to deal with the summations directly. We calculate the infinite summations in the above expressions with a reasonable high cutoff using MATHEMATICA [31].

TABLE I. The saturation values $\Sigma^2_{\rm sat}$ from the expression in Eq. (26) and the numerical data in Fig. 3. $\Sigma^2_{\rm sat}$ from numerical data is estimated as the arithmetic mean of $\Sigma^2(r)$ over $r \in [500 - 4000]$. The corresponding error bars represent the standard deviation of the mean from original data.

| | $\Sigma^2_{\rm sat}$ [Eq. (26)] | $\Sigma^2_{\rm sat}$ (from numerical data) |
|---|---|---|
| **COE ⊗ COE** | 29.01 | 28.99(7) |
| **CUE ⊗ CUE** | 20.26 | 20.25(4) |
| **CSE ⊗ CSE** | 17.73 | 17.74(25) |

In Figs. 3(a)–3(c), the numerical results of $\Sigma^2(r)$ for all three classes COE ⊗ COE, CUE ⊗ CUE, and CSE ⊗ CSE are shown. The numerical data for different classes has good agreement with the respective analytical expressions [Eqs. (30)–(32)]. $\Sigma^2(r)$ for small intervals is displayed in the insets. The linear growth of $\Sigma^2(r)$ in different insets exhibits the uncorrelated nature of eigenangles, irrespective of the different classes. The saturation behavior of $\Sigma^2(r)$ at large $r$ can be clearly observed in the main frames. To become more quantitative, we estimate the saturation values from numerical data and mention them in Table I. These are consistent with the values obtained from the infinite series in Eq. (26). One can also see that the saturation values are different for all classes, indicating the different degrees of level repulsion as in the symmetry classes of circular ensembles.

We have separately verified the linear growth and the saturation behavior of $\Sigma^2(r)$ for the direct product of three independent random unitary matrices. For the sake of brevity, we refrain from presenting this detailed data here. Albeit, for completeness, we show in Fig. 4 the data of $\Sigma^2(r)$ vs $r$ for small intervals. One can notice that with the increase in $m$ the regime of linear growth of $\Sigma^2(r)$ is also extended. In case of $m = 2\,(N = 100)$, $\Sigma^2(r) \sim r$ only up to $\lesssim 10$ (see

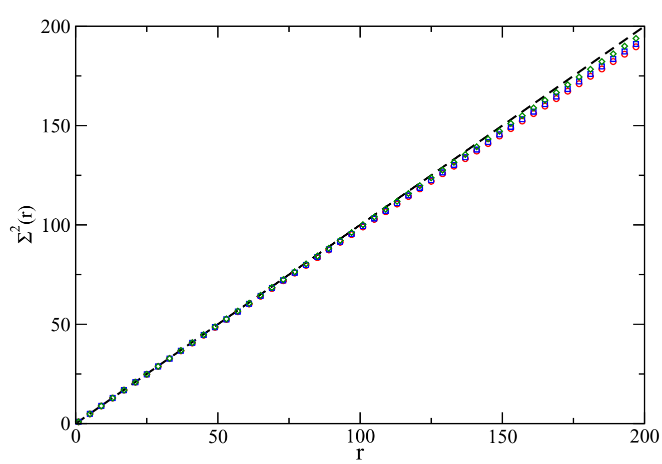


FIG. 4. Number variance $\Sigma^2(r)$ versus interval size $r$ for direct product of three independent random unitary matrices drawn from COE (circle), CUE (square), and CSE (diamond), respectively. The size of the spectrum is $N^3 = 100^3$. The dashed line indicates $\Sigma^2(r) = r$.

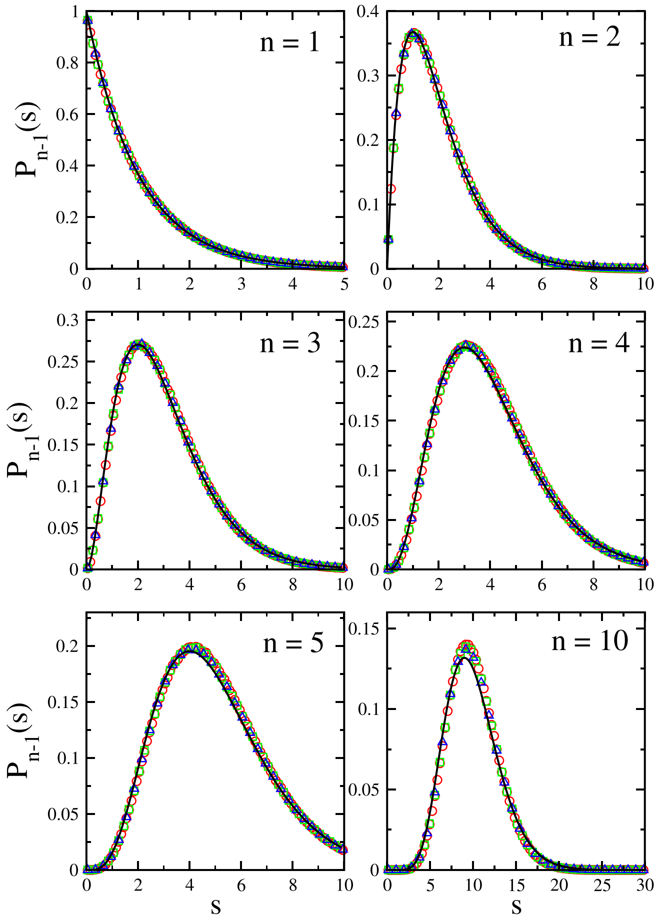


FIG. 5. Level-spacing distribution $P_{n-1}(s)$ for different values of $n$ (see keys). The different symbols circle, square, and diamond in the same panel represent numerical data for COE $\otimes$ COE, CUE $\otimes$ CUE, and CSE $\otimes$ CSE, respectively. The size of the spectrum is $N^2 = 100^2$. The solid curve in different panels denotes Poisson distribution [Eq. (33)].

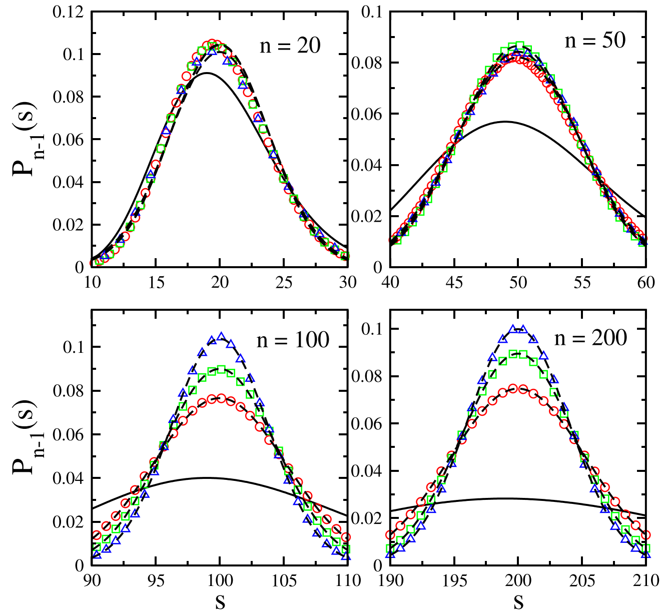


FIG. 6. Level-spacing distribution $P_{n-1}(s)$ for different values of $n$ (see keys). The symbols circle, square, and diamond in the same panel represent numerical data for COE $\otimes$ COE, CUE $\otimes$ CUE, and CSE $\otimes$ CSE, respectively. The size of the spectrum is $N^2 = 100^2$. The dashed curves represent Gaussian distribution plotted using Eq. (34). The solid curves denote Poisson distribution [Eq. (33)].

Fig. 3), while for $m = 3\,(N = 100)$ the present figure shows that $\Sigma^2(r) \sim r$ at least up to $\lesssim 100$, a fact that $\Sigma^2(r) \sim r$ for $r \ll N^{m-1}$ predicted in Sec. IV.

### B. Level-spacing distribution

The $n$th nearest-neighbor spacing distribution for a sequence of uncorrelated levels is *Poisson distribution* [3],

$$P(n; s) = \frac{s^{n-1}}{(n-1)!} \exp(-s), \tag{33}$$

where the variance of the distribution is $n$. We have seen above that the eigenangles in the spectrum from direct product ensembles are uncorrelated for interval size $r \ll N^{m-1}$. It is, therefore, expected that the level-spacing distribution $P_{n-1}(s)$ should be Poissonian for $n \leqslant r$. This behavior was proved for the direct product of two large CUE matrices in Ref. [15].

In Fig. 5, we numerically calculate $P_{n-1}(s)$ for different classes (COE $\otimes$ COE, CUE $\otimes$ CUE, CSE $\otimes$ CSE) and different values of $n$. When $n$ is small $(= 1, 2, 3, 4)$, $P_{n-1}(s)$ for all three classes has nice agreement with Poisson distribution. However, with increase in $n$, the deviations from Poisson begin (see panels for $n = 5, 10$ in the same figure). These deviations arise due to the long-range correlations in the spectrum. One should note that the variance of distribution $P_{n-1}(s)$ is similar to the number variance $\Sigma^2(r)$ and will cease to increase at large $n$. The large spacings in a spectrum are the sum of several consecutive level spacings. We expect from the *central limit theorem* that the level-spacing distribution, with increase in $n$, will tend to a *Gaussian distribution*:

$$G(s) = \frac{1}{\sqrt{2\pi\sigma^2}} \exp\left(-\frac{(s-\mu)^2}{2\sigma^2}\right). \tag{34}$$

In Fig. 6, $P_{n-1}(s)$ are calculated for $n = 20, 50, 100, 200$. The dashed curves are plotted from Eq. (34) with mean $\mu$ and variance $\sigma^2$ determined from the numerical data. One can clearly see the deviation from Poisson distribution. While, with increase in $n$, $P_{n-1}(s)$ is approached to Gaussian distribution. Especially, at very large $n\,(= 100, 200)$, the agreement of numerical data of distribution $P_{n-1}(s)$ and Gaussian is excellent.

## VI. MULTIPARTITE SYSTEM OF QUANTUM KICKED ROTORS

We now discuss a composite system [32] constructed by the noninteracting QKRs, where the spectral properties of the above discussed direct product ensembles may be realized. The QKR is a paradigmatic example of quantum chaos, whose spectral statistics mimic RMT-behavior. The time-evolution operator of QKR can be represented by an $N$-dimensional matrix in position basis [18,33]

$$\mathcal{U}_{kl} = \frac{1}{N}\exp\left[-i\alpha\left\{\cos\left(\frac{2\pi k}{N}+\theta_0\right)\right\}\right] \times \sum_{n=-(N-1)/2}^{(N-1)/2}\exp\left[-i\left(\frac{n^2}{2}-\lambda n-2\pi n\frac{(k-l)}{N}\right)\right], \tag{35}$$

where $\alpha$ is the kicking parameter that brings nonintegrability in QKR, and parameters $\lambda$ and $\theta_0$ control the time-reversal and parity symmetry breaking, respectively. When $\alpha \gg N$, with setting $\theta_0 \neq 0$ and $\lambda = 0$ the eigenangle spectrum of the matrix $\mathcal{U}$ exhibits local fluctuations similar to those of the COE matrix. Further, if $\lambda \neq 0$ too, the fluctuations correspond to the CUE class. Here, we construct a multipartite system of independent QKRs. Let $H_1, H_2, ...., H_m$ be the Hamiltonians of QKRs, each defined in $N$-dimensional Hilbert space. Then, the total Hamiltonian of the multipartite QKR system is given by

$$H = H_1 \otimes \mathbb{I} + \mathbb{I} \otimes H_2 + ..... + \mathbb{I} \otimes H_m, \tag{36}$$

which is defined in $N^m$-dimensional Hilbert space. The time-evolution operator for this system is expressed as

$$\widetilde{\mathcal{U}} = \mathcal{U}_1 \otimes \mathcal{U}_2 \otimes ..... \otimes \mathcal{U}_m. \tag{37}$$

It is clear that the operators $\mathcal{U}_1, \mathcal{U}_2, ...$ are the time-evolution operators of independent QKRs. When writing in a generic basis, $\widetilde{\mathcal{U}}$ takes the form of a matrix obtained from the direct product of component matrices $\mathcal{U}_1, \mathcal{U}_2, ...$ each belonging to a circular ensemble.

We numerically investigate the spectral properties of the multipartite QKR system with $m = 2$. The size of individual QKR matrices is $N = 101$. To obtain good accuracy in the statistics, we constructed an ensemble of 1000 independent realizations of the multipartite QKR system by setting the parameter $\alpha = j\alpha_0 + (i-1)\Delta$ in Eq. (35) with $\alpha_0 = 50\,000$, $\Delta = 25\,000$, and $j = 1, 2, ..., 1000$. The index $i$ runs over the members of a multipartite system $(i = 1, 2)$ to ensure their independence. We have two possible cases to investigate, one when $\lambda = 0$, and another when $\lambda \neq 0$. For $\lambda = 0$, the spectral statistics of the multipartite QKR system should be equivalent to that of the direct product of independent random unitary matrices from COE, while for $\lambda \neq 0$ it should be equivalent to the direct product of independent random unitary matrices from CUE.

In Figs. 7(a)–7(b), the number variance $\Sigma^2(r)$ for $\lambda = 0$ and $\lambda = 0.9$ is calculated. When the width of the interval $r$ is small, $\Sigma^2(r) \sim r$ for both cases (see insets), describing the Poissonian behavior of the spectral statistics. Similar to our direct product ensembles, the strong level repulsion in the spectrum is developed at large $r$, indicated by the saturation of $\Sigma^2(r)$ in the main frames of the figure. The data are also in good agreement with the analytical expressions [Eqs. (30) and (31)] obtained in Sec. V. It implies the plausibility of the direct product ensembles.

The other quantity, level-spacing distribution, also has features similar to the ensembles of direct product of independent random unitary matrices. Again, for the sake of brevity, we did not present those data here.

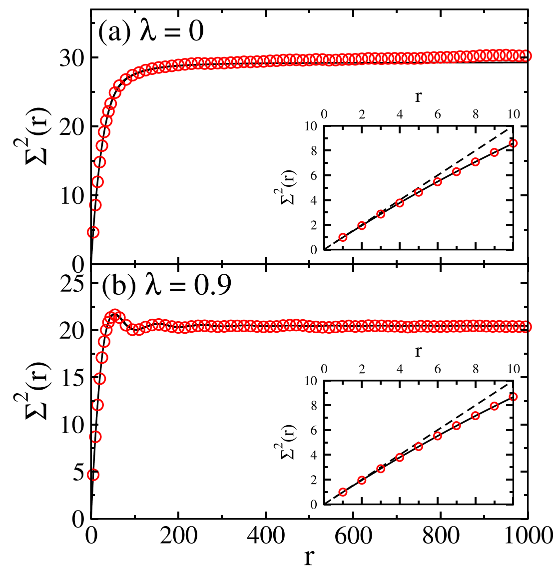


FIG. 7. Plot of number variance $\Sigma^2(r)$ vs interval size $r$ for (a) $\lambda = 0$, (b) $\lambda = 0.9$. The size of the spectrum obtained from the direct product of independent matrices is $N^2 = 101^2$. Numerical data for small $r$ is given in insets, where the dashed lines indicate $\Sigma^2(r) = r$. The solid curves in main frame and inset of (a) and (b) are plotted using Eqs. (30) and (31), respectively.

## VII. SUMMARY AND DISCUSSION

We now conclude this paper with a summary and discussion of our results. The random unitary matrices from circular ensembles are considerably used to model the spectral fluctuations of complex quantum systems. With the reach of the field to a wide variety of systems, different generalized ensembles of random unitary matrices have also been proposed in the literature. The ensemble composed by the direct product of random unitary matrices is one of them. In this paper, we have studied in detail the ensemble of a direct product of $m$ independent random unitary matrices of size $N$ drawn from a given circular ensemble. We investigated the two-point level correlations and fluctuation properties of the eigenangle spectrum. The analytical results are presented for the direct product of $m$ independent random unitary matrices of size $N$ in general, and their numerical verification is provided for $m = 2$ and $N = 100$.

An important statistical measure to investigate the two-point level correlations is the number variance $\Sigma^2(r)$. It can be calculated in terms of the form factor $C(p)$. We found that the form factor $C^{m\otimes}(p)$ of direct product of $m$ independent random unitary matrices is simply the $m$th power of the form factor $C(p)$ of random unitary matrices. Using this relation, we were able to see that the number variance $\Sigma^2(r) \sim r$ for interval size $r \ll N^{m-1}$, i.e., the eigenangles are uncorrelated in the intervals of size $r \ll N^{m-1}$. Another important observation from this relation $C^{m\otimes}(p) = [C(p)]^m$ is that the form factor $C^{m\otimes}(p)$ is suppressed at small values of index $p$. With the illustration of a model proposed by Berry [23] and Serota and Wickramasinghe [24], we showed that the suppression of the form factor at small $p$ (short wave number) results in the saturation of $\Sigma^2(r)$ at large $r$. It further implies the presence of strong correlations between the distant eigenangles of the spectrum.

We numerically verified the linear growth of number variance $\Sigma^2(r)$ for direct product of two independent random unitary matrices. The numerical data further verified the saturation behavior of $\Sigma^2(r)$ at large $r$. We also numerically calculated the $n$th nearest-neighbor spacing distribution $P_{n-1}(s)$. For small spacings, $P_{n-1}(s)$ is Poissonian showing agreement with the linear variation of $\Sigma^2(r)$ at small $r$. For large spacings, $P_{n-1}(s)$ has non-Poissonian behavior. In fact, with increase in $n$, $P_{n-1}(s)$ tends to the Gaussian distribution.

Finally, we demonstrated a multipartite system of independent QKRs. The spectral statistics of this composite system shows good agreement with our findings for direct product ensembles. Such direct product ensembles of random unitary matrices have applications in quantum information theory, wireless networks, etc.


## ACKNOWLEDGMENT

R.A. would like to thank Sanjay Puri for useful discussions.



[1] F. J. Dyson, J. Math. Phys. **3**, 140 (1962).
[2] T. A. Brody, J. Flores, J. B. French, P. A. Mello, A. Pandey, and S. S. M. Wong, Rev. Mod. Phys. **53**, 385 (1981).
[3] M. L. Mehta, *Random Matrices*, Pure and Applied Mathematics, Vol. 142 (Elsevier Science, Amsterdam, 2004).
[4] F. Haake, *Quantum Signatures of Chaos*, Springer Series in Synergetics, Vol. 54 (Springer-Verlag, Berlin, 2010).
[5] H. Stöckmann, *Quantum Chaos: An Introduction* (Cambridge University Press, Cambridge, UK, 1999).
[6] G. Akemann, J. Baik, and P. D. Francesco, *The Oxford Handbook of Random Matrix Theory* (Oxford University Press, New York, 2011).
[7] C. W. J. Beenakker, Rev. Mod. Phys. **69**, 731 (1997).
[8] T. Guhr, A. Muller-Groeling, and H. A. Weidenmüller, Phys. Rep. **299**, 189 (1998).
[9] F. J. Dyson, J. Math. Phys. **3**, 1199 (1962).
[10] A. Lakshminarayan, Z. Puchała, and K. Życzkowski, Phys. Rev. A **90**, 032303 (2014).
[11] P. Kondratiuk and K. Zyczkowski, Acta Phys. Pol. A **124**, 1098 (2013).
[12] S. C. L. Srivastava, S. Tomsovic, A. Lakshminarayan, R. Ketzmerick, and A. Bäcker, Phys. Rev. Lett. **116**, 054101 (2016).
[13] T. Herrmann, M. F. I. Kieler, F. Fritzsch, and A. Bäcker, Phys. Rev. E **101**, 022221 (2020).
[14] J. J. Pulikkottil, A. Lakshminarayan, S. C. L. Srivastava, A. Bäcker, and S. Tomsovic, Phys. Rev. E **101**, 032212 (2020).
[15] T. Tkocz, M. Smaczyński, M. Kuś, O. Zeitouni, and K. Życzkowski, Random Matrices: Theor Appl. **1**, 1250009 (2012).
[16] M. Smaczyński, T. Tkocz, M. Kuś, and K. Życzkowski, Phys. Rev. E **88**, 052902 (2013).
[17] G. Casati, B. V. Chirikov, F. M. Izraelev, and J. Ford, in *Stochastic Behavior in Classical and Quantum Hamiltonian Systems*, edited by G. Casati and J. Ford (Springer, Berlin, 1979), pp. 334–352.
[18] F. M. Izrailev, Phys. Rep. **196**, 299 (1990).
[19] A. Pandey, S. Puri, and S. Kumar, Phys. Rev. E **71**, 066210 (2005).
[20] A. Pandey, Ann. Phys. **119**, 170 (1979).
[21] More precisely, this timescale is $N$ for COE or CUE matrices of size $N$ and $2N$ for CSE matrices of size $2N$ due to Kramers degeneracy. See Ref. [19].
[22] G. Casati, B. V. Chirikov, and I. Guarneri, Phys. Rev. Lett. **54**, 1350 (1985).
[23] M. V. Berry, Proc. R. Soc. London A **400**, 229 (1985).
[24] R. Serota and J. Wickramasinghe, Int. J. Mod. Phys. B **16**, 4649 (2002).
[25] A. Bäcker, F. Steiner, and P. Stifter, Phys. Rev. E **52**, 2463 (1995).
[26] M. Robnik and G. Veble, J. Phys. A: Math. Gen. **31**, 4669 (1998).
[27] R. Prakash and A. Pandey, Phys. Rev. E **93**, 052225 (2016).
[28] F. Mezzadri, Notices Am. Math. Soc. **54**, 592 (2007).
[29] J. Maziero, Front. ICT **3**, 4 (2016).
[30] E. Anderson, Z. Bai, C. Bischof, S. Blackford, J. Demmel, J. Dongarra, J. Du Croz, A. Greenbaum, S. Hammarling, A. McKenney, and D. Sorensen, *LAPACK Users' Guide*, 3rd ed. (Society for Industrial and Applied Mathematics, Philadelphia, PA, 1999).
[31] Wolfram Research, Inc., Mathematica, Version 11.1, Champaign, IL (2017).
[32] H. Breuer and F. Petruccione, *The Theory of Open Quantum Systems* (Oxford University Press, New York, 2002).
[33] F. M. Izrailev, Phys. Rev. Lett. **56**, 541 (1986).